ARMY RESEARCH LABORATORY

Nanostructuring of Aluminum Alloy Powders by Cryogenic Attrition with Hydrogen-Free Process Control Agent

by Frank Kellogg, Clara Hofmeister, Anit Giri, and Kyu Cho

ARL-TR-7208 **February 2015**

NOTICES

Disclaimers

The findings in this report are not to be construed as an official Department of the Army position unless so designated by other authorized documents.

Citation of manufacturer's or trade names does not constitute an official endorsement or approval of the use thereof.

Destroy this report when it is no longer needed. Do not return it to the originator.

Army Research Laboratory
Aberdeen Proving Ground, MD 21005-5069

ARL-TR-7208 **February 2015**

Nanostructuring of Aluminum Alloy Powders by Cryogenic Attrition with Hydrogen-Free Process Control Agent

Frank Kellogg
Bowhead Science and Technology

Clara Hofmeister
Advanced Materials Processing and Analysis Center, Department of Materials Science and Engineering, University of Central Florida

Anit Giri
TKC Global

Kyu Cho
Weapons and Materials Research Directorate, ARL

REPORT DOCUMENTATION PAGE	Form Approved OMB No. 0704-0188

1. REPORT DATE *(DD-MM-YYYY)*	2. REPORT TYPE	3. DATES COVERED (From - To)
February 2015	Final	July 2013–August 2014

4. TITLE AND SUBTITLE
Nanostructuring of Aluminum Alloy Powders by Cryogenic Attrition with Hydrogen-Free Process Control Agent

5a. CONTRACT NUMBER

5b. GRANT NUMBER

5c. PROGRAM ELEMENT NUMBER

6. AUTHOR(S)
Frank Kellogg, Clara Hofmeister, Anit Giri, and Kyu Cho

5d. PROJECT NUMBER

5e. TASK NUMBER

5f. WORK UNIT NUMBER

7. PERFORMING ORGANIZATION NAME(S) AND ADDRESS(ES)
US Army Research Laboratory
ATTN: RDRL-WMM-D
Aberdeen Proving Ground, MD 21005-5069

8. PERFORMING ORGANIZATION REPORT NUMBER
ARL-TR-7208

9. SPONSORING/MONITORING AGENCY NAME(S) AND ADDRESS(ES)

10. SPONSOR/MONITOR'S ACRONYM(S)

11. SPONSOR/MONITOR'S REPORT NUMBER(S)

12. DISTRIBUTION/AVAILABILITY STATEMENT
Approved for public release; distribution is unlimited.

13. SUPPLEMENTARY NOTES

14. ABSTRACT
Aluminum 5083 powder was milled through cryogenic attrition for 8, 16, and 24 h with graphite as a hydrogen-free process control agent. The powders were degassed to remove moisture and other impurities. The degassed powders have a relatively low hydrogen concentration. The morphology, grain sizes, and stability of the milled powders were compared, and it was found that while there was little difference in grain size between the 3 milling times, powders milled for 16 and 24 h showed more grain stability than powders milled for 8 h.

15. SUBJECT TERMS
cryogenic attrition, PCA, nanostructuring, hydrogen, cryomilling

16. SECURITY CLASSIFICATION OF:			17. LIMITATION OF ABSTRACT	18. NUMBER OF PAGES	19a. NAME OF RESPONSIBLE PERSON
a. REPORT	b. ABSTRACT	c. THIS PAGE			Kyu Cho
Unclassified	Unclassified	Unclassified	UU	22	19b. TELEPHONE NUMBER (*Include area code*) (410) 306-0820

Standard Form 298 (Rev. 8/98)
Prescribed by ANSI Std. Z39.18CC

Contents

List of Figures

List of Tables

Acknowledgments

The authors would like to give special thanks to Brady Butler for lending his expertise to gathering and interpreting the X-ray diffraction data.

INTENTIONALLY LEFT BLANK.

1. Introduction

The combination of low weight and high strength make aluminum (Al) and its alloys attractive materials in the development of new structures and systems employed by the US Army. The effectiveness of Al alloys can be further enhanced, by increases in strength and ductility, through the development of bulk nanograined microstructures. Powder metallurgy techniques can be used to develop bulk nanograined materials through the consolidation of nanograined powders. The development of the nanograined powder can be attained through multiple processing routes, but one of the more promising ways is through cryogenic attrition. One form of cryogenic attrition is low-energy grinding of conventional (micron-sized) powder with milling media (typically stainless steel balls) in liquid nitrogen (LN_2).[1] Cryogenic attrition, also called cryomilling (both terms will be used interchangeably in this report), has several advantages: 1) it can create large particle agglomerates consisting of nanograined powder, ensuring safe powder handling; 2) attrition in LN_2 prevents sample contamination from oxygen and/or moisture; and 3) it can cause the formation of N inclusions that behave as grain stabilizers.[2] Absorption of N via cryogenic attrition in LN_2 resulted in high stability of the microstructure, such that the nanograins barely increased in size even after heat treatment or thermo-mechanical processing (TMP) at elevated temperatures. There is experimental evidence and theoretical models that suggest that N reacts with Al, leading to incorporation of N at surfaces and interfaces.[3] Incorporation of N can enhance the strength of the composite by solid solution strengthening as well as by dispersion strengthening or the Orowan strengthening mechanism.[4]

In cryomilling, a process control agent (PCA) is necessary to prevent excessive cold welding of the powders. However, PCAs introduce contaminants that have to be removed after milling to allow for clean and strong interfacial bonding between the nanostructured particles during TMP to transform the powders into bulk form. The removal process, known as degassing, is done by heating the powders to high temperature under vacuum. Recently we have explored using various PCAs and studied their effect on the mechanical response of trimodal Al metal matrix composites.[5] Most of the PCAs commonly used (e.g., stearic acid, oleic acid, caprylic acid) contain carbon and hydrogen (H). It is important to have as little H as possible in the structural material to avoid brittleness.[6–8] Hydrogen is difficult to get rid of during the degassing process, and a H-free surfactant is desirable for use in cryogenic attrition. Preliminary research was initiated under an Army Small Business Innovation Research effort using graphite as a PCA during cryomilling [Delahanty T, Pittsburgh Materials Technology, personal communication, 2012 Jan.]. In this research we have employed graphite as a PCA that contains no H in order to reduce H concentration in the cryomilled powders after the degassing process. The degassing process allows for the possibility of grain growth for nanostructured Al and subsequent degradation of mechanical properties.

Absorption of N via cryogenic attrition in LN_2 imparts stability to the microstructure such that the nanograins do not grow in size even after heat treatment or TMP at elevated temperatures. Therefore it is also important that we are able to retain as high an amount of N after degassing as possible. We performed cryogenic attrition of Al5083 powders for 8, 16, and 24 h with graphite as a PCA to study the effect of milling time on the microstructure, phases present, impurity concentrations (H and N) and stability of the powders upon degassing.

2. Experiment

A Szegvari Union Process 1-S attritor (Fig. 1) modified to allow for continuous flow of LN_2 was used for cryogenic attrition of Al5083 (–325 mesh, Valimet, Inc). The Al5083 powder (800 g) was cryomilled in LN_2 for 8, 16 and 24 h with a ball-to-powder weight ratio of 32:1. Graphite powder (0.15 wt%, Alfa Aesar) was V-blended with the Al5083 powder prior to cryogenic attrition to ensure a uniform distribution of PCA. Prior to adding the powder, the attritor tank was filled with LN_2 and flushed 3 times for cleanliness. The tank was then refilled, allowing the temperature to stabilize at the operating temperature (–196 °C), after which the powder was added for runs of 8, 16, or 24 h. After cryogenic attrition, the powder and LN_2 slurry was collected in a stainless steel bucket. The mill was purged with LN_2 several times to collect as much powder as possible. The bucket was then put into a controlled atmosphere glove box to protect the powder as the LN_2 boiled off. The powders were degassed at 410 °C in a custom-made static vacuum degasser (Fig. 2) with a maximum vacuum of approximately 10^{-6} Torr. Once high vacuum was achieved, the furnace was ramped to the desired temperature over 6 h, soaked for 8 h, and then allowed to cool to room temperature. Table 1 lists the powders that were milled and degassed during these experiments.

Fig. 1 The Szegvari attritor available at the US Army Research Laboratory (ARL), modified to enable cryogenic attrition

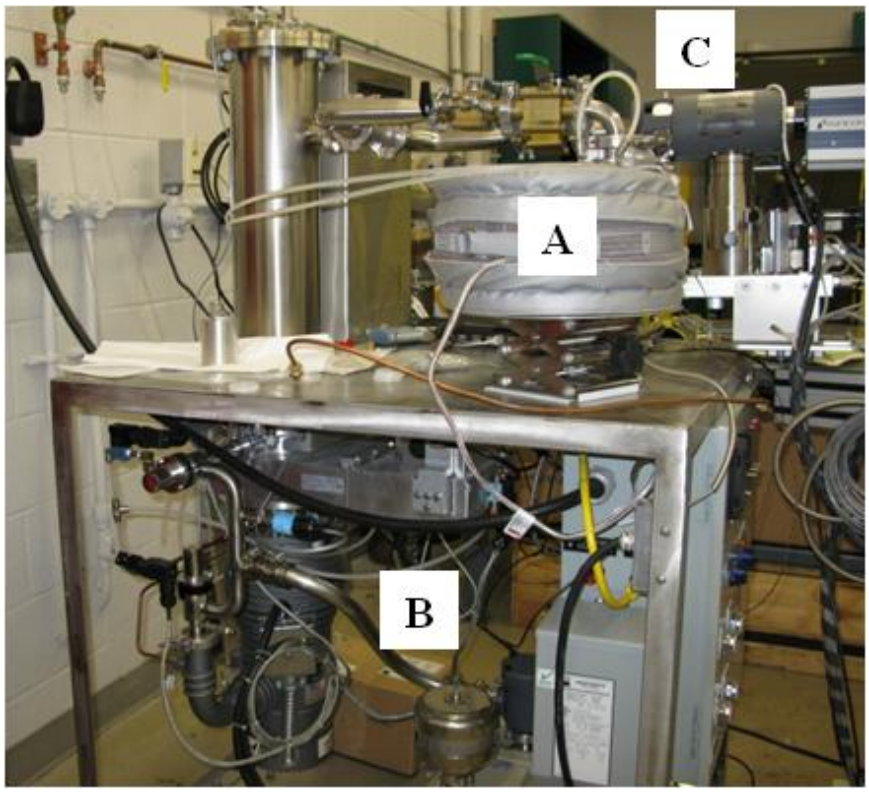

Fig. 2 ARL degassing system. Powder was added to a metal canister and wrapped with a heater band (A). The vacuum system (B) then evacuated the canister to draw off volatiles and hinder oxidation. The mass spectroscopy system (C) may be used to identify volatiles boiled off by the sample.

Table 1 Powder samples examined

Sample ID	Milling Time (h)	Notes
Al5083	Not milled	As received
8CM	8	Cryomilled 8 h
8CMD	8	Cryomilled 8 h and degassed at 410 °C for 8 h
16CM-1	16	Cryomilled 16 h
16CMD-1	16	Cryomilled 16 h and degassed at 410 °C for 8 h
24CM-1	24	Cryomilled 24 h
24CM-2	24	Cryomilled 24 h
24CM-3	24	Cryomilled 24 h
24CMD-1	24	Cryomilled 24 h and degassed at 410 °C for 8 h

The milled powders were characterized for morphology, microstructure, and chemistry. An Hitachi S4700 field emission scanning electron microscope (FESEM) was used to examine particle morphology after milling. A Leco ONH 836 inert gas fusion and thermal conductivity elemental analyzer was used to determine how much N and H were incorporated into the powder during the milling process. The crystallite size of the powders and identification of precipitates were determined using X-ray diffraction (XRD) via the Williamson/Hall method.[9–13]

3. Results and Discussion

3.1 FESEM Characterization

The starting powder was examined using FESEM to determine the initial microstructure (Fig. 3). The powder is spherical in shape and unagglomerated with a particle size range of approximately 0.5–20 μm.

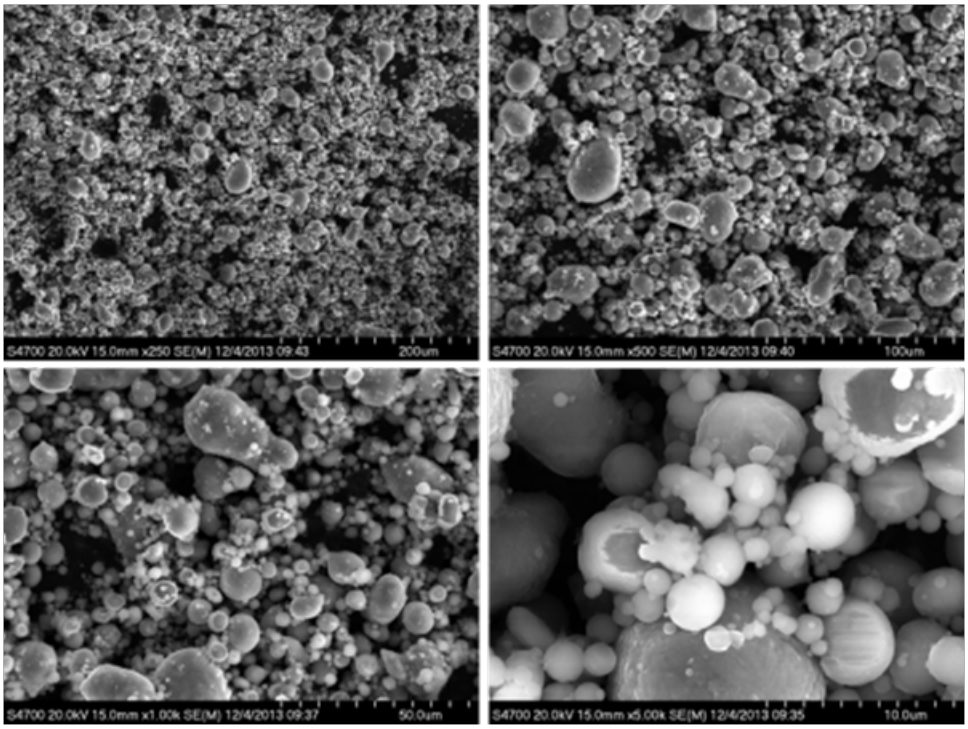

Fig. 3 FESEM micrographs of the starting Al5083 powder

After 8 h of attrition, the shape of the particles became angular, the surface roughened, and the particles agglomerated (see Fig. 4). There are negligible observable differences in the size, morphology, and texture of milled Al agglomerates between samples milled for 8, 16, or 24 h (Fig. 5). This indicates that before or at 8 h of cryomilling time, there is a balance in the rate of the respective fracturing and cold welding of the powders.

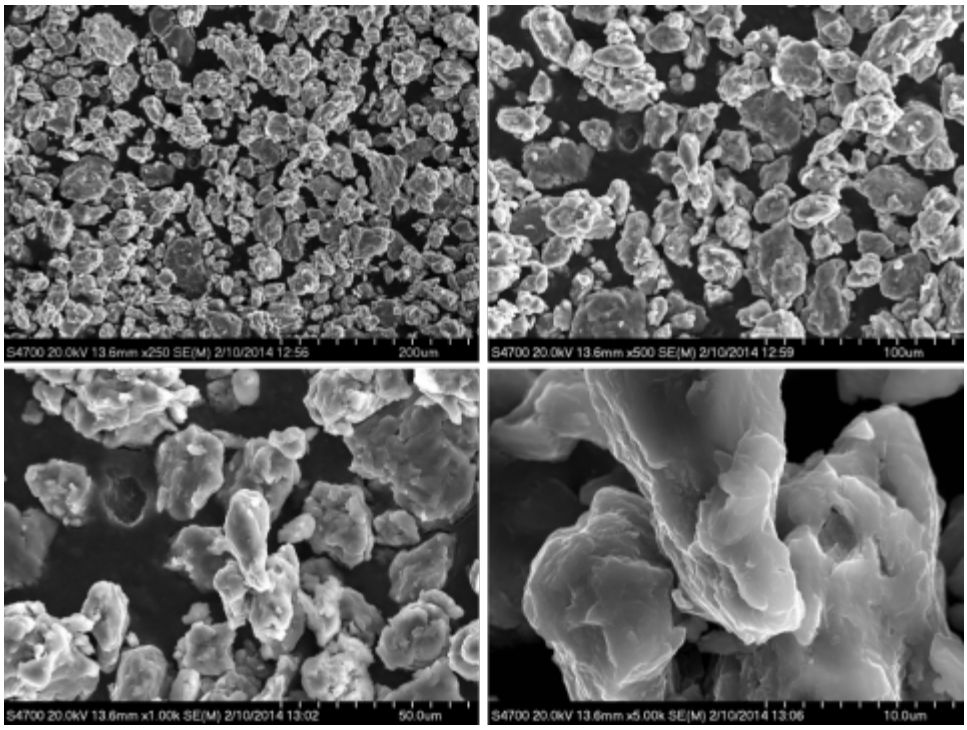

Fig. 4 FESEM micrographs of 8-h cryomilled (8CM) powder

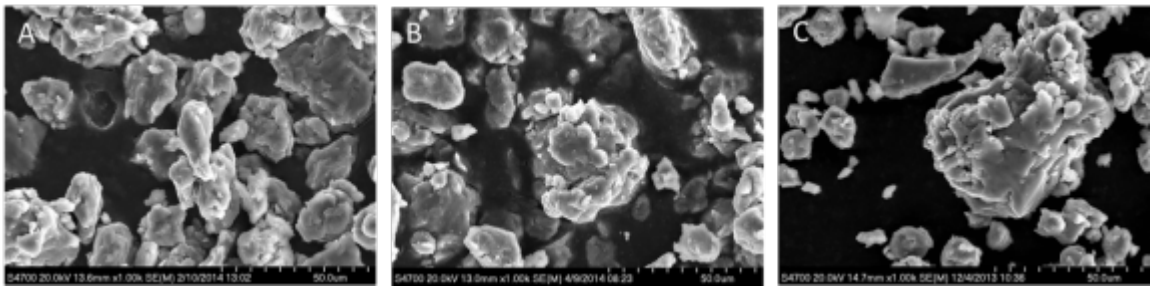

Fig. 5 Comparison of agglomerate morphology of the powders cryomilled for 8, 16 or 24 h. Micrograph (A) is of 8CM, (B) is 16CM-1, and (C) is 24CM-2.

Three batches of powder underwent cryogenic attrition for 24 h: 24CM-1, 24CM-2, and 24CM-3 (Fig. 6). All 3 batches of the 24-h milled powders exhibit similar size and shape; therefore, the morphological changes from cryogenic attrition are repeatable from run to run.

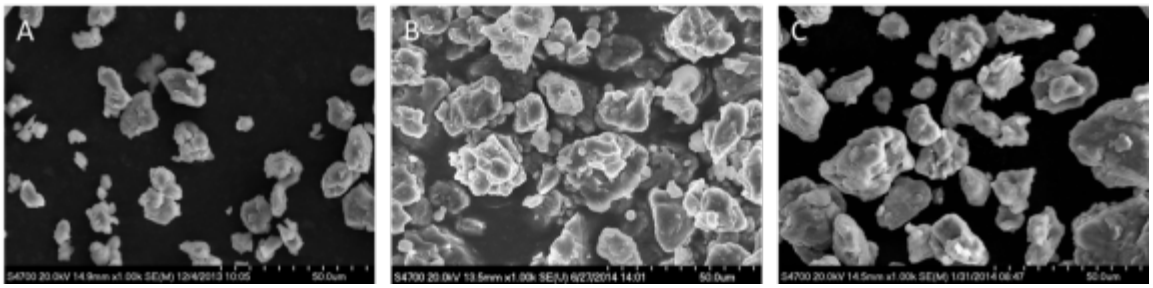

Fig. 6 Comparison of powders produced by 3 different 24-h cryomilling runs

Powder was also degassed at 410 °C after cryogenic attrition for 8, 16 and 24 h (8CMD, 16CMD-1, and 24CMD-1; Fig. 7). Overall, there was no sintering observed. The morphology, size, and texture of the powders did not change with degassing.

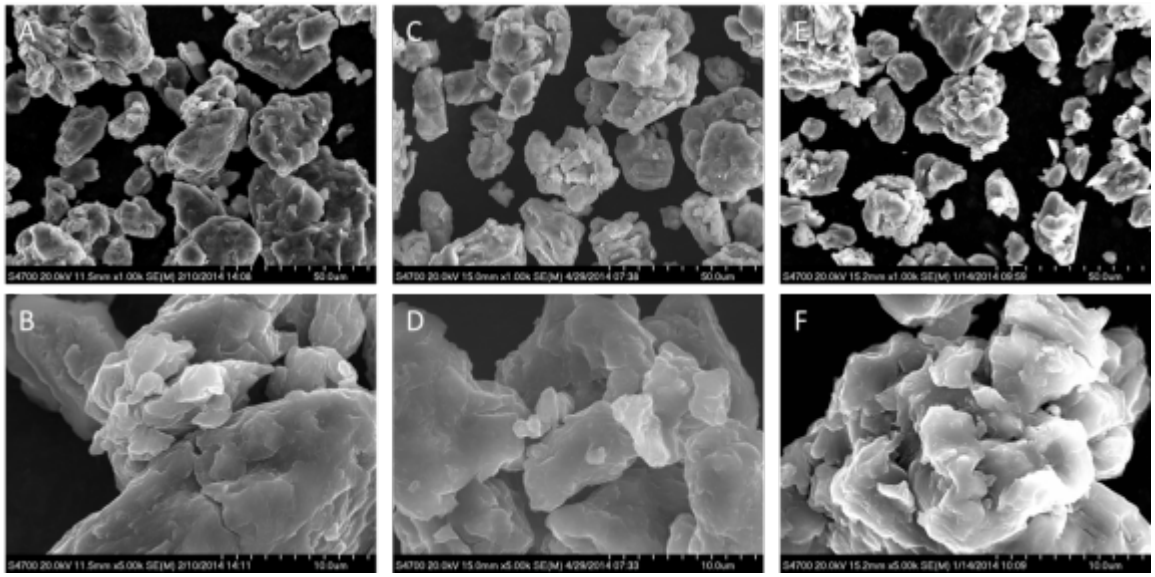

Fig. 7 Comparison of powders degassed at 410 °C as a function of milling time: A and B are micrographs of 8CMD; C and D are micrographs of 16CMD-1; and E and F are micrographs of 24CMD-1.

There was no observable difference in the size or morphology between the powders cryomilled for various times and degassed.

3.2 Elemental Analysis

The results from the gas fusion chemical analysis are collected in Figs. 8 and 9. Figure 8 shows the H concentration of as-cryomilled powders and the degassed powders. The 8-h cryomilled powder had 540 ppm of H. The same powder was used under the same milling conditions, but with 14.3-wt% boron carbide (B_4C) using stearic acid as a PCA, had an H concentration of 1,000 ppm [Delahanty T, Pittsburgh Materials Technology, personal communication, 2012 Jan.]. The reduced H concentration in our sample might be the result of employing an H-free PCA. The H concentration was further reduced to 50 ppm after

degassing at 410 °C for 8 h. In this context, recognize that cold-pressed and high-strain-rate-extruded samples, containing trimodal metal matrix composite consisting of unmilled Al5083 and 8-h cryomilled powders of Al5083 and B_4C with stearic acid as a PCA and degassed at 410 °C, contained 90-ppm H; this is almost double the amount of H obtained in the 8-h milled and degassed powders processed in this research. Usually degassed powder, after going through primary consolidation and TMP, contains less H than just degassed powder. The relatively lower H content in the powders produced in this research could be ascribed to the use of graphite as a PCA.

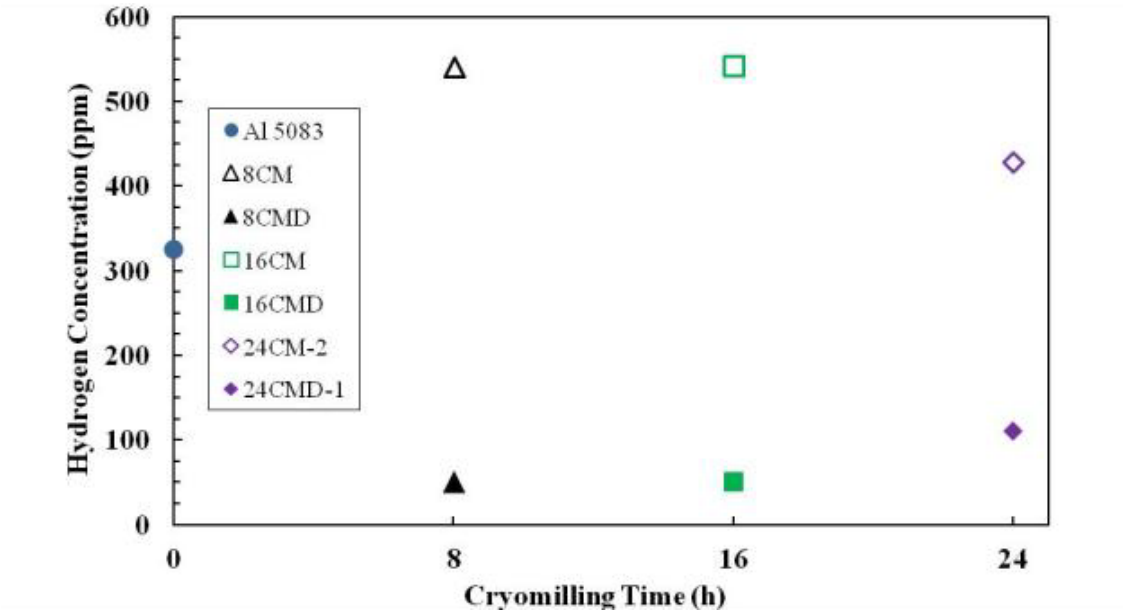

Fig. 8 Hydrogen concentration of cryomilled and degassed powders

Figure 9 shows a linear increase in N concentration with milling time; Ye et al.[14] reported an N concentration of 0.4 wt% for 8-h cryomilled Al5083 powder with stearic acid as a PCA. Hashemi-Sadraei[15] also reported similar N concentrations (e.g., 0.9 wt% and 1.9 wt%, respectively) for 8- and 24-h cryomilled Al5083 and 14.3-wt% B_4C composites using stearic acid as a PCA. Degassing the powders does not alter the N concentration of the powders significantly. As mentioned, maintaining the N level is important, as this is the basis for forming the small nanodispersoids that give cryomilled Al its grain stability during sintering and results in improved mechanical response.

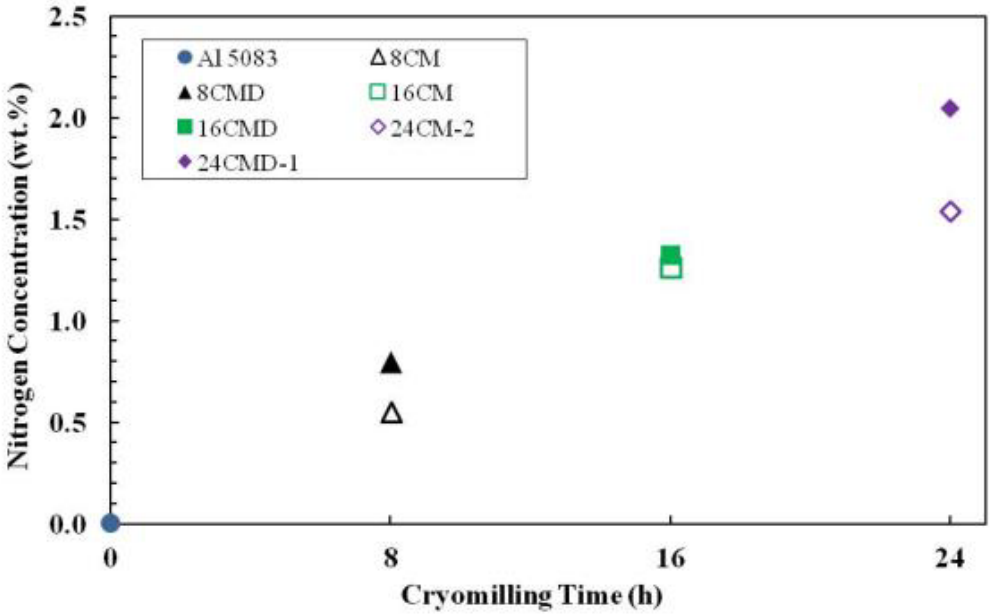

Fig. 9 Nitrogen concentration of milled and degassed powders

3.3 X-ray Diffraction

The XRD patterns of the cryomilled powder samples are shown in Fig. 10. Cryogenic attrition did not introduce any contaminates or produce phase changes that could be detected via XRD.

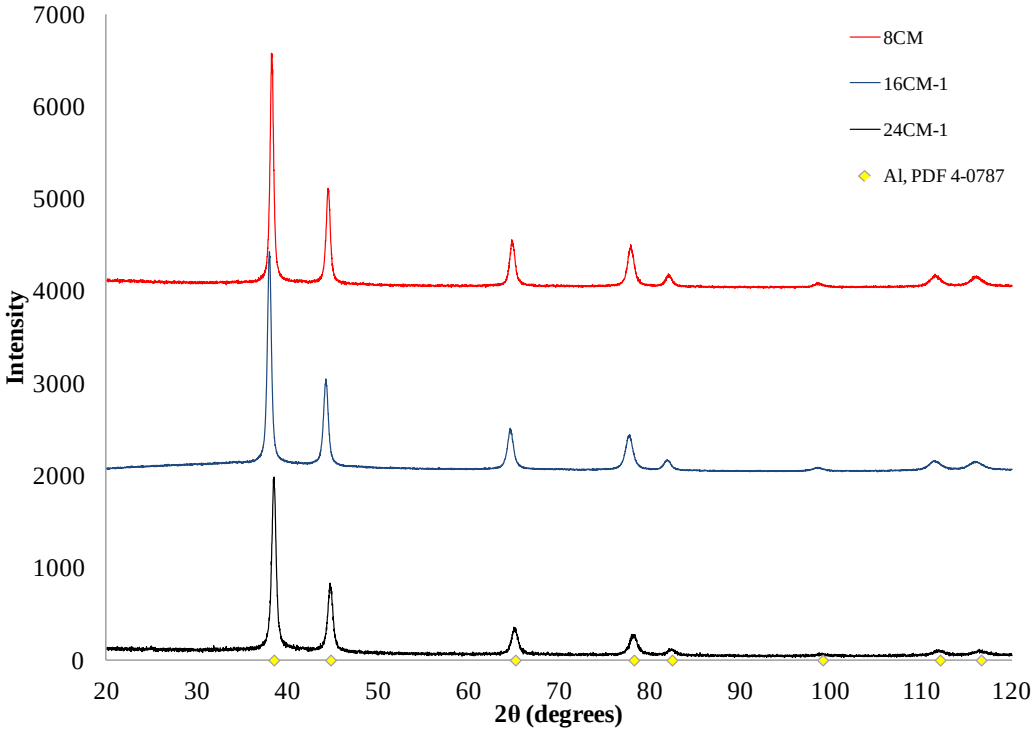

Fig. 10 XRD patterns for the cryomilled Al powders as a function of milling time

All of the degassed powders show additional peaks primarily between 2θ = 30° and 50° (θ is Bragg angle) (Fig. 11), which could be ascribed to Al-manganese (Mn) alloy Al_6Mn. This phase has been previously identified in degassed cryomilled Al5083 powder and has been found in as-cast parts made from Al5083 powder.[5]

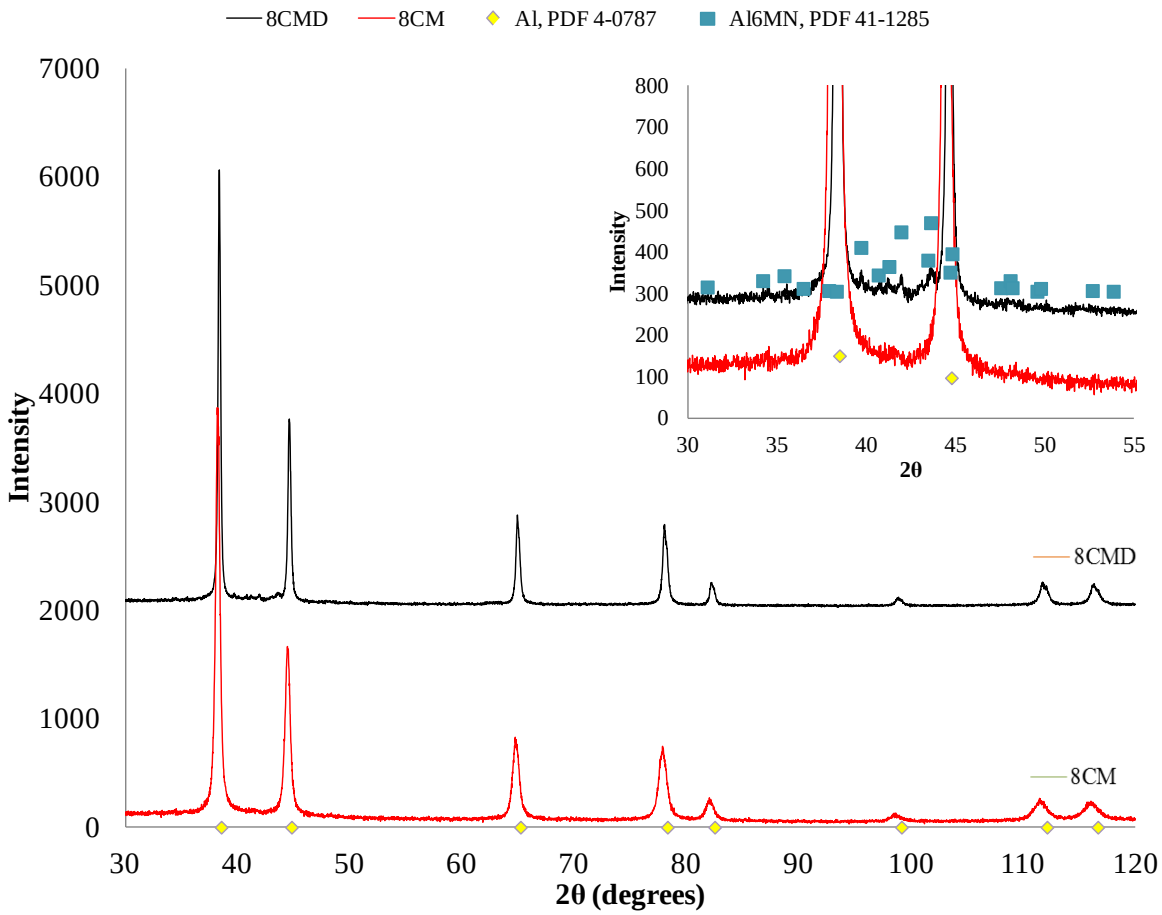

Fig. 11 XRD patterns for the degassed Al powders

The crystallite size and microstrain were calculated from the XRD profile based off of the Williamson/Hall method.[9–13] This method follows Eq. 1 (derived from the Scherrer formula),

$$H\cos\theta = \frac{K\lambda}{G} + 4\varepsilon\sin\theta, \quad (1)$$

where H is the full width at half maximum of the XRD peaks (as obtained through the pseudo-Voigt fitting procedure), K is the Scherrer constant (varies between 0.9 and 1.0), λ is the wavelength of the X-ray radiation, G is grain size, and ε is microstrain. The full width at half maximum is influenced by the line broadening of the XRD spectra, which is caused by the material having small grains, strain, and machine broadening. The Williamson/Hall equation can be used to isolate the size and strain effects but cannot account for machine broadening; this can be done by running a standard material that does not show line broadening such as lanthanum hexaboride (LaB_6) or, as in this report, cerium(IV) oxide (CeO_2, or ceria). To determine the full width at half maximum, each peak is fit with a pseudo-Voigt function (where 2w is full width at half maximum).

$$V_p(x) = \eta L(x) + (1-\eta)G(x) \text{ with } 0 < \eta < 1, \quad (2)$$

$$L(x) = \frac{1}{1+(\frac{x-x_o}{w})^2}, \quad (3)$$

and

$$G(x) = \exp\left((-\ln(2))(\frac{x-x_o}{w})^2\right). \quad (4)$$

After fitting, the calculated full widths at half maximum can be modeled using the Caglioti equation,

$$H = (UTan^2\theta + VTan\theta + W)^2, \quad (5)$$

which can then be plugged into the Williamson/Hall equation and solved for both grain size and microstrain. While this method is a relatively easy and straight-forward way for calculating grain sizes and microstrains (especially with the right software), the results are only as good as the calculated fits of the data. A poor or improper fit could lead to erroneous measurements.[12,13]

For the 8-h cryomilled sample, the calculated grain size is 44 nm. The grain size decreased to 34 nm for the 16-h cryomilled powder and remained the same for the 24-h cryomilled powder. Degassing led to increases in grain size for the 8- and 24-h milled powders. The crystallite size for the 8-h degassed sample was calculated to be greater than 100 nm. The crystallite size measurement is valid only if the crystallite size remains below 100 nm; because coarse grains do not contribute to peak broadening, large grains are not accounted for in these measurements. XRD may report an artificially small grain size.[9] The 24-h cryomilled and degassed powder had smaller grain sizes than the corresponding 8-h samples. This could indicate that the thermal stability of the grains resulting from enhanced concentrations of N species imparted during milling. There was no change in grain size after degassing for the 16-h sample. Grain size analysis via transmission electron microscopy is necessary to explain this and is currently being conducted. The microstrain for the 16-h sample is greater than that of 8-h sample and remains practically unchanged for the 24-h sample. The microstrain decreases after degassing due to strain relaxation. The results of XRD analysis are detailed in Table 2.

Table 2 Grain size and strain measured via XRD line profile analysis

Sample	Crystallite size (nm)	Strain (%)
8CM	44	0.36
8CM	>100[a]	0.22
8CM	34	0.41
16CMD-1	34	0.27
24CM-2	33	0.43
24CMD-1	65	0.33

[a]Any calculated value over 100 nm is invalid with this technique.

4. Conclusions

To explore the applicability of employing an H-free PCA in cryomilling with a view to reducing the H content in Al-based lightweight structural alloys, Al5083 powders were subjected to cryogenic attrition for 8, 16, and 24 h with graphite as a PCA. The powders were degassed to remove moisture and other contaminants introduced during cryogenic attrition. The H content of the degassed powders reduced significantly after degassing due to moisture removal and was relatively low compared with those produced using H-containing surfactants. Nitrogen concentration increases with increasing cryogenic attrition time and is not altered by degassing. There were insignificant differences found in the agglomerate size, morphology, or texture regardless of cryogenic attrition time or degassing treatment. There were few to no differences found in the crystallite sizes between the as-milled samples. The only differences arose after degassing, where the powder milled for 8 h experienced more grain growth and exhibited less grain stability than the powder milled for 16 or 24 h. This suggests that cryogenic attrition for at least 16 h could lead to powders that can retain their nanograin sizes at higher sintering temperatures, leading to better consolidation and improved performance for parts made from nanograin cryomilled powder. Detailed experiments using the primary and secondary TMPed samples made from the cryomilled and degassed powders along with their microstructural characterizations will be performed to study the effect of H and N content on mechanical response and the results published soon.

5. References

1. Witkin DB, Lavernia EJ. Synthesis and mechanical behavior of nanostructured materials via cryomilling. Progress in Materials Science. 2006;51(1):1–60.
2. Hofmeister C, Yao B, Sohn Y, Delahanty T, van den Bergh M, Cho K. Composition and structure of nitrogen-containing dispersoids in trimodal aluminum metal-matrix composites. Journal of Materials Science. 2010;45:4871–4876.
3. Vogt RG, Zhang Z, Topping TD, Lavernia EJ, Schoenung JM. J Mater Process Technol. 2009;209:5046.
4. Li Y, Liu W, Ortalan V, Li WF, Zhang Z, Vogt R, Browning ND, Lavernia EJ, Schoenung JM. HRTEM and EELS study of aluminum nitride in nanostructured Al 5083/B_4C processed via cryomilling. Acta Mater. 2010;58:1732.
5. Hofmeister C, Giri A, Brennan S, Sohn YH, Delahanty T, Cho K. Effect of process control agent on the microstructure and mechanical behavior of an aluminum and B_4C metal matrix composite. In: Grandfield J, editor. Light metals 2014. Wiley Online; 2014 Feb 4. p.1343–1346. [accessed 2015 Jan 28]. DOI: 10.1002/9781118888438.ch224.
6. Hampton M, Schur D, Zaginaichenko S, Trefilov V. Hydrogen materials science and chemistry of metal hydride. In: Proceedings of the NATO Advanced Research Workshop on Hydrogen Materials Science and Chemistry of Metal Hydride; 1999; Katsiveli, Ukraine. New York (NY): Springer NATO Science Series; c1999.
7. Ambat R, Dwarakadasa E. Effect of hydrogen in aluminum and aluminum alloys: a review Bull Mater Sci. 1996;19(1):103–114.
8. Louthan M. Hydrogen embrittlement of metals: a primer for the failure analyst. Washington (DC): Department of Energy (US); 2008. DOE Report No.: WSRC-STI-2008-00062.
9. Zhang Z, Zhou F, Lavernia EJ. On the analysis of grain size in bulk nanocrystalline materials via x-ray diffraction. Metallurgical and Materials Transactions A. 2003;34:1349–1355.
10. Liu K, Mücklich F. Thermal stability of nano-RuAl produced by mechanical alloying. Acta Materialia. 2001;49(3):395–403.
11. Natter H, Schmelzer M, Löffler M, C Krill, Fitch A, Hemplemann R. Grain-growth kinetics of nanocrystalline iron studied in situ by sycnchrotron real-time x-ray diffraction. J Phys Chem B. 2000;104(11):2467–2476.

12. He J, Ye J, Lavernia E, Matejczyk D, Bampton C, Schoenung J. Quantitative analysis of grain size in bimodal powders by x-ray diffraction and transmission electron microscopy. J Mater Sci. 2004;39:6957–6964.

13. Balzar D. X-ray diffraction line broadening: modeling and applications to high T_c superconductors. J Research N.I.S.T. 1993;98(3):321–353.

14. Ye J, He J, Schoenung J. Cryomilling for the fabrication of a particulate B_4C reinforced Al nanocomposite: part I. effects of process condition on structure. Metall Mater Trans A. 2006;37:3099–3109.

15. Hashemi-Sadraei L, Mousavi S, Vogt R, Li Y, Zhang Z, Lavernia E, Schoenung J. Influence of nitrogen content on thermal stability and grain growth kinetics of cryomilled aluminum composites. Metall Mater Trans A. 2012;43(2):747–756.

1 (PDF) DEFENSE TECHNICAL INFORMATION CTR DTIC OCA

2 (PDF) DIRECTOR US ARMY RESEARCH LAB RDRL CIO LL IMAL HRA MAIL & RECORDS MGMT

1 (PDF) GOVT PRINTG OFC A MALHOTRA

1 (PDF) DIRECTOR US ARMY RESEARCH LAB AMSRD ARL WM MB A FRYDMAN

2 (PDF) BENET LABS AMSTA AR CCB E KATHE A LITTLEFIELD

3 (PDF) DARPA J GOLDWASSER M MAHER N WIEDENMAN

2 (PDF) US ARMY TACOM TARDEC AMSTA TR C FILAR J KOSHKO

60 (PDF) DIR USARL
RDRL VTP
E CHIN
RDRL WM
P BAKER
B FORCH
S KARNA
RDRL WML
M ZOLTOSKI
RDRL WML A
W OBERLE
RDRL WML B
R PESCE-RODRIGUEZ
B RICE
N TRIVEDI
RDRL WML C
S AUBERT
RDRL WML D
R BEYER
RDRL WML E
P WIENACHT
RDRL WML F
M IIG
RDRL WML G
J SOUTH
RDRL WML H
J NEWILL
B SCHUSTER
RDRL WMM
J BEATTY
R DOWDING
J ZABINSKI
RDRL WMM A
J SANDS
J TZENG
E WETZEL
RDRL WMM B
T BOGETTI
B CHEESEMAN
C FOUNTZOULAS
G GAZONAS
D HOPKINS
T JENKINS
B LOVE
P MOY
B POWERS
C RANDOW
T SANO
R WILDMAN
C YEN
RDRL WMM C
J LA SCALA
RDRL WMM D
R CARTER
K CHO
A GIRI
M PEPI
S WALSH
RDRL WMM E
J ADAMS
M COLE
J SINGH
J SWAB
RDRL WMM F
S GRENDAHL
L KECSKES
E KLIER
H MAUPIN
E KLIER
RDRL WMM G
A RAWLETT

RDRL WMP
D LYON
S SCHOENFELD
RDRL WMP A
R MUDD
RDRL WMP B
C HOPPEL
RDRL WMP C
T BJERKE
RDRL WMP D
J RUNYEON
RDRL WMP E
P SWOBODA
RDRL WMP F
N GNIAZDOWSKI
RDRL WMP G
N ELDREDGE